Proceedings of the 2018 IEEE
International Conference on Robotics and Biomimetics
December 12-15, 2018, Kuala Lumpur, Malaysia

# CombX: Design of a Haptic Device for Teleoperation*

Bin Zhao, Shu'an Zhang, Zhonghao Wu, Qi Li and Kai Xu, *Member, IEEE*

***Abstract*— A haptic device which can provide force and torque outputs is preferred in teleoperation, virtual reality, etc. The dilemma for researchers is that such a haptic device is not easily accessible: the commercial products are expensive to buy, while the state-of-the-art research prototypes are difficult to reproduce outside the original laboratories. This paper presents the design and preliminary experimentation of a haptic device, the CombX, with both force and torque outputs. The CombX is constructed from two TouchX haptic devices that only generate force outputs at their styluses. Since the TouchX's original stylus does not allow effective connection between two TouchX devices, a new stylus is carefully designed and fabricated via 3D printing, to replace the original styluses. An optimization for determining the arrangement of the two TouchX devices was performed to maximize the workspace. Positioning precisions and orientation workspace of the CombX were experimentally examined. The future work mainly includes the calibration and characterizations of the CombX's force and torque output capabilities, in order to fully verify the effectiveness of the proposed idea.**

## I. Introduction

Haptic devices are utilized for generating kinesthetic interaction between a user and real/simulated environments. Via forces, vibrations and/or motions, the haptic device can recreate the touch sense to the user. Their specific uses would affect their forms and involve different theoretical foundations [1]. A haptic device is often used at the master side in teleoperation systems to sense the positions and orientations of its end effector as well as provide kinesthetic interactions with the operator.

According to the abilities of the sensing inputs and the force-torque outputs, the existing haptic devices that may be applied in teleoperation tasks can be classified as follows.

- 3-in-3-out designs: they measure 3-DoF (Degree of Freedom) inputs (usually positions) and provide 3-DoF outputs (usually forces). Commercial products include the delta.3 and the omega.3 devices (Force Dimension), and the Novint Falcon (Novint Technologies). Research prototypes include the joystick mechanism [2], the DELTA-R device [3] and the SHaDe device [4] that senses the orientation and generates torque outputs.
- 6-in-3-out designs: they sense 6-DoF inputs (positions and orientations) and provide 3-DoF outputs (usually forces). The Touch and TouchX devices (3D Systems) and the omega.6 device (Force Dimension) are popular products.
- 6-in-n-out designs: they measure 6-DoF inputs and generate multi-DoF outputs (some or all forces and torques components). Early research prototypes include the haptic devices [5, 6] with hybrid serial-parallel structures. The products include the delta.7 and sigma.7 devices (Force Dimension) and the Phantom Premium (3D Systems). These products are relatively expensive. On the other hand, researchers developed many 6-in-n-out devices, such as the haptic pen [7], the VISHARD6 [8], the PATHOS-II [9], the haptic cobot [10], the modified DELTA-R device [3], the pinch–grasp haptic interface [11], and the VirtuaPower device [12].

Please note that an addition end effector, such as a gripper, can always be integrated to the stylus of a haptic device, leading to the increase of the number of the device's DoFs. This additional DoF is not counted in the above classification.

Teleoperation applications prefer 6-in-n-out haptic devices since they give the operator a realistic sense of the external wrenches. However, these 6-in-n-out devices are not easily accessible, because the commercial ones are usually expensive (unit price above USD $50,000) and it is difficult to reproduce the research prototypes outside the laboratories where the devices were originally developed.

The design of a cost-effective 6-in-5-out haptic device, the CombX, is hence proposed in this paper. As shown in Fig. 1, the CombX is constructed from two TouchX devices (3D Systems). The core motivation is to introduce a haptic device which has relatively high cost-performance and is still relatively simple to build. What's more, the CombX device with this serial-parallel hybrid structure can probably better achieve a proper balance between the workspace and stiffness, since a serial-structured haptic device usually has a larger workspace and a parallel-structured haptic device has better stiffness and force output capability.

Referring to Fig. 1, the CombX consists of two TouchX devices to provide force and torque outputs, while each TouchX device only generates force outputs. The TouchX's original stylus does not allow effective connection between two such units. A new stylus was carefully designed and fabricated via 3D printing, to replace the original styluses and connect the two TouchX devices. The arrangement of the two TouchX devices was optimized to maximize the CombX's workspace.

Similar ideas of combining two Novint Falcon devices or two Omni devices to provide 5-dimensional wrench outputs were reported in [13] and [14] respectively. The connection and the arrangement were not optimized and the resultant

*This work was supported in part by the National Natural Science Foundation of China (Grant No. 51435010, Grant No. 51722507 and Grant No. 91648103), and in part by National Key R&D Program of China (Grant No. 2017YFC0110800).

Bin Zhao, Shu'an Zhang and Zhonghao Wu are with the RII Lab (Lab of Robotics Innovation and Intervention), UM-SJTU Joint Institute, Shanghai Jiao Tong University, Shanghai, China (emails: zhaobin2014@sjtu.edu.cn, jimmyonthego@sjtu.edu.cn and zhonghao.wu@sjtu.edu.cn).

Qi Li and Kai Xu are with School of Mechanical Engineering, Shanghai Jiao Tong University, Shanghai, China (emails: liqi362202@sjtu.edu.cn, k.xu@sjtu.edu.cn; corresponding author: K. Xu).

978-1-7281-0377-8/18/$31.00 © 

workspace can hardly satisfy the requirements of a teleoperation task. An optimized design of combining two Omni devices was proposed in [15]. However, the optimized arrangement often interfaces with the operator's arm and made the device's use inconvenient. Furthermore, the TouchX has a better force output capability than that of the Omni device so that the CombX would have better output performances. It is expected that the CombX would find applications in robot-assisted surgeries, virtual reality, and other human-machine interactions.

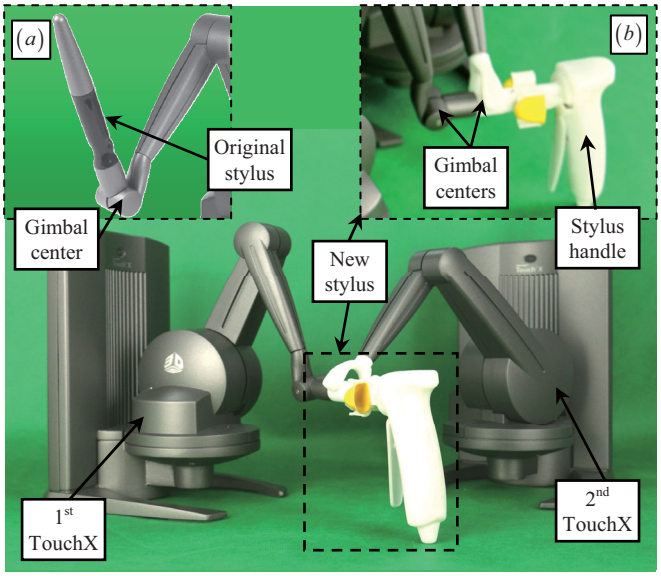


Figure 1. The CombX device: (a) the original stylus, and (b) the new stylus

This paper is organized as follows. The design construction of the CombX is described in Section II. Section III presents the kinematics model and the arrangement optimization of the CombX device. Preliminary experimental characterizations are elaborated in Section IV, with the conclusions and future work summarized in Section V.

## II. System Description of The CombX

A TouchX has six revolute joints: three proximal ones are active while the three distal ones are passive. It can generate a force at its Gimbal center using its three active joints. Then the orientation of its stylus with respect to the Gimbal center, as indicated in Fig. 1(a), is sensed by the three potentiometers in its distal joints.

Referring to Fig. 1(b), when two TouchX devices are connected, each TouchX exerts a force at the Gimbal center of the new stylus, resulting in a 3-dimensional force output and a 2-dimensional torque output. The torque component about the axis of the new stylus cannot be generated.

Since the CombX is constructed from two TouchX devices, its workspace heavily depends on how the two TouchX devices are connected. It is clear that the orientation workspace of the CombX will be more severely restricted by the TouchX's workspace, if the two gimbal centers, indicated in Fig. 1(b), are located further apart.

In theory, if the two gimbal centers coincide, the CombX's orientation workspace will not be affected. But due to practical limitations, the distance $L$ between the two gimbal centers is designed as 40 mm as shown in Fig. 3.

In order to minimize the modifications to the TouchX devices, it was decided that the 1st TouchX would be responsible for sensing the position and orientation of the CombX's new stylus. Hence, only a part of the original stylus was removed, reserving the 6th potentiometer to be connected with the new stylus, as shown in Fig. 2.

The 2nd TouchX is expected to cooperate with the 1st one to generate force and torque outputs. And the orientation sensing of the 2nd TouchX's stylus is no longer needed for the CombX. Therefore, its distal structures were disassembled. An arch fork and a shaft sleeve were used for connecting with the new stylus.

The new stylus hence includes a handle for housing all the electric components of the two TouchX devices, a clutch trigger, a pair of pinch triggers, a shaft sleeve, an arch fork, etc.

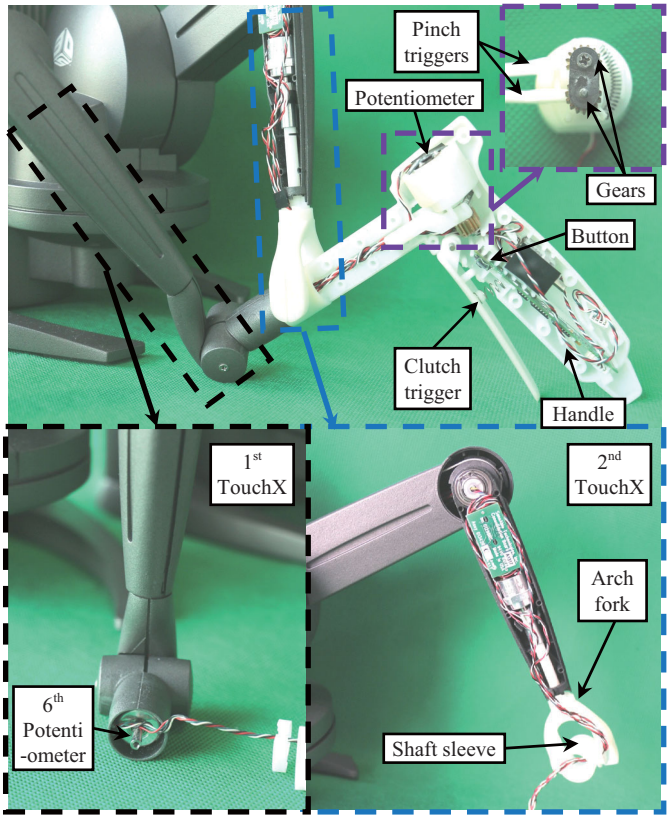


Figure 2. The cutaway-view of CombX

There is a button board in the TouchX's original stylus. Hence the handle of the new stylus will house the two button boards, and the two potentiometers of the 2nd TouchX. Please note the integrity of the TouchX's electrics system is fully preserved.

The clutch trigger is spring loaded. Once pulled, a push-key button will be pressed by the clutch trigger. If the CombX is used in a teleoperation, this clutch trigger can be used to establish or cut off a connection with the remote system. A pair of pinch triggers is installed to the axes of a pair of meshing gears. Then, the opening angle of the pinch triggers can be sensed by one potentiometer that is originally inside the

2nd TouchX device. The reading from this potentiometer can be used to control the opening angle of a gripper in the remote manipulator during teleoperation.

The shaft sleeve is installed on the shaft of the new stylus as shown in Fig. 2. The shaft sleeve can also rotate freely with respect to the arch fork. The arch fork is connected with the 4th potentiometer of the 2nd TouchX device. It was designed to have a rotation range as large as possible for the handle and the shaft sleeve.

Relative positioning of the two TouchX devices is determined via an optimization as in Section III.C. Referring to the relative positioning, the CombX is mounted on an acrylic board, as shown in Fig. 5.

## III. Modeling and Optimization of The CombX

### A. Nomenclatures and Coordinates

As shown in Fig. 3, the kinematics of the CombX is described by the following coordinates.

- *World Coordinate* $\{W\} \equiv \{\hat{\mathbf{x}}_W, \hat{\mathbf{y}}_W, \hat{\mathbf{z}}_W\}$ is located at the base of the CombX.
- *TouchX Device Coordinates* $\{Dij\} \equiv \{\hat{\mathbf{x}}_{Dij}, \hat{\mathbf{y}}_{Dij}, \hat{\mathbf{z}}_{Dij}\}$ ($i = 1, 2; j = 0, 1, 2, \cdots, 6$) are assigned to the base or the $j^{th}$ link of the $i^{th}$ TouchX device according to the Denavit-Hartenberg rules as shown in Fig. 3(b). The XY-plane of the World Coordinate $\{W\}$ is coplanar with the XY-plane of the TouchX device base coordinate $\{Di0\}$. In Fig. 3(b), the Y axes of the $\{Dij\}$ are hidden to display the coordinates clearly.
- *Handle Coordinates* $\{H\} \equiv \{\hat{\mathbf{x}}_H, \hat{\mathbf{y}}_H, \hat{\mathbf{z}}_H\}$ is assigned to the CombX's handle of the new stylus. The $\{H\}$ is parallel with the $\{D16\}$ and located at ${}^{D16}\mathbf{p}_H = [0 \text{ mm } 0 \text{ mm } L/2 \text{ mm}]^T$ in $\{D16\}$. $L$ is the distance between the origins of $\{D16\}$ and $\{D26\}$.

### B. Maintaining the Integrity of the Specifications

As shown in Fig. 3(b), the kinematics of one TouchX device can be easily described by assigning seven coordinates. Referring to the Denavit-Hartenberg rules, the homogeneous transformation matrix of the adjacent coordinates is as follows.

$$ {}^{Di(j-1)}\mathbf{T}_{Dij} = \begin{bmatrix} {}^{Di(j-1)}\mathbf{R}_{Dij} & {}^{Di(j-1)}\mathbf{p} \\ \mathbf{0}_{1\times3} & 1 \end{bmatrix}, \; i = 1, 2, j = 1, 2, \cdots, 6 \quad (1) $$

Where $ {}^{Di(j-1)}\mathbf{R}_{Dij} = \begin{bmatrix} \cos\theta_{ij} & -\sin\theta_{ij} & 0 \\ \sin\theta_{ij}\cos\alpha_{j-1} & \cos\theta_{ij}\cos\alpha_{j-1} & -\sin\alpha_{j-1} \\ \sin\theta_{ij}\sin\alpha_{j-1} & \cos\theta_{ij}\sin\alpha_{j-1} & \cos\alpha_{j-1} \end{bmatrix} $

and $ {}^{Di(j-1)}\mathbf{p} = \begin{bmatrix} a_{j-1} & -d_j\sin\alpha_{j-1} & d_j\cos\alpha_{j-1} \end{bmatrix}^T $.

The kinematics of the TouchX devices from $\{Di6\}$ to $\{Di0\}$ can be formulated in (2).

$$ {}^{Di0}\mathbf{T}_{Di6} = \prod_{j=1}^{6} {}^{Di(j-1)}\mathbf{T}_{Dij}, \; i = 1, 2, j = 1, 2, \cdots, 6 \quad (2) $$

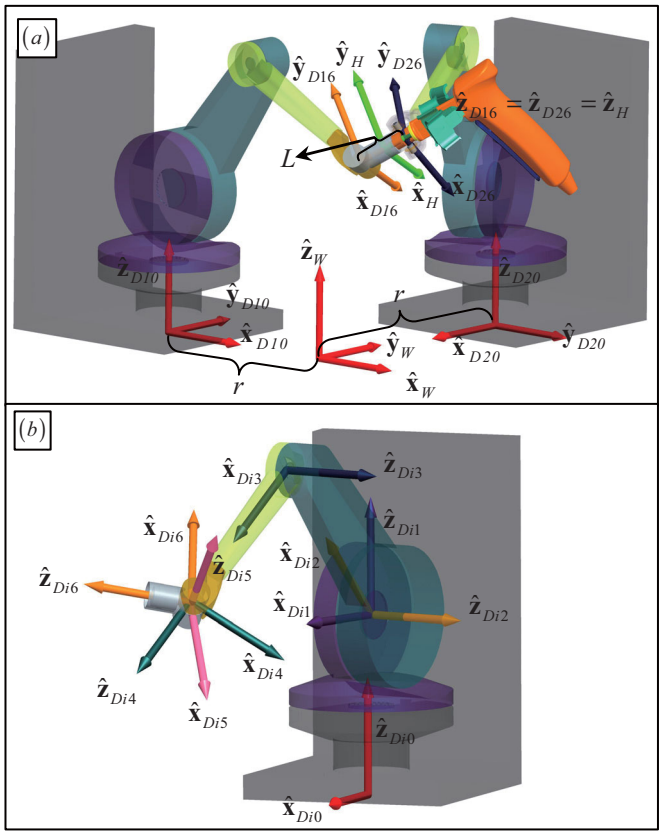


Figure 3. Coordinates assignment: (a) coordinates of the CombX, and (b) coordinates of one TouchX device

Because the 1st TouchX is utilized for sensing the position and orientation of the new stylus, the handle coordinate $\{H\}$ is described in the 1st TouchX device base coordinate $\{D10\}$. The transformation matrix from $\{H\}$ to $\{D10\}$ is as in (3).

$$ {}^{D10}\mathbf{T}_H = {}^{D10}\mathbf{T}_{D16} \cdot \begin{bmatrix} \mathbf{I}_{3\times3} & {}^{D16}\mathbf{p}_H \\ \mathbf{0}_{1\times3} & 1 \end{bmatrix} \quad (3) $$

The detailed Denavit-Hartenberg parameters of one TouchX device are shown in TABLE I.

TABLE I. Denavit-Harttenberg Parameters of the TouchX

| Index $j$ | Parameters and Value Ranges | | | |
|---|---|---|---|---|
| | $\alpha_{j-1}$ | $a_{j-1}$ | $d_j$ | $\theta_{ij}$ |
| 1 | 0° | 0 | 120mm | $\theta_{i1} \in$ [-53°, 53°] |
| 2 | -90° | 0 | 0 | $\theta_{i2} \in$ [-100°, 0°] |
| 3 | 0° | 135mm | 0 | $\theta_{i3} \in$ [110°, 235°] |
| 4 | 90° | 0 | 132mm | $\theta_{i4} \in$ [-126.5°, 126.5°] |
| 5 | -90° | 0 | 0 | $\theta_{i5} \in$ [-137°, -4°] |
| 6 | 90° | 0 | 0 | $\theta_{i6} \in$ [-150°, 150°] |

### C. Optimized Arrangement of the Two TouchX Devices

The arrangement optimization to efficiently utilize the TouchX devices' translational workspace determines their relative positioning with respect to each other. For the convenience in assembly and use, the two TouchX devices are assumed to be placed on the same plane and the $\hat{\mathrm{x}}_{D10}$ and $\hat{\mathrm{x}}_{D20}$ are intersected at the origin of $\{W\}$. The distance between the origins of $\{W\}$ and $\{D10\}$ is equal to the distance between those of $\{W\}$ and $\{D20\}$. $\{D10\}$ is parallel with $\{W\}$ and the $\hat{\mathrm{x}}_{W}$ is coaxial with $\hat{\mathrm{x}}_{D10}$. Then two arrangement parameters describes the relative position as follows: 1) $r$: the distance between the origins of $\{W\}$ and $\{D10\}$ or $\{D20\}$, and 2) $\gamma$: the rotational angle from $\{D20\}$ to $\{D10\}$.

The optimal arrangement was implemented to obtain the relative position of the TouchX devices with the largest workspace of the CombX. To quantify the CombX's workspace, the number of the valid poses of $\{H\}$ is counted for every pair of the $r$ and $\gamma$ values. For the given $r$ and $\gamma$, the valid pose of $\{H\}$ for the CombX satisfies two conditions: 1) The corresponding position $\{D16\}$ can be obtained with respect to the given $\{H\}$. For this $\{D16\}$ pose, the joints values of the 1st TouchX device are within the joint ranges. 2) The corresponding origin position of $\{D24\}$ can be calculated with respect to the given $\{H\}$. The origin position of $\{D24\}$ is located in the workspace of the 2nd TouchX device.

The positions to be tested are uniformly distributed within a cubic volume of 600 mm × 600 mm × 600 mm whose center is located at the origin of $\{W\}$ with the intervals of 2 mm in the XYZ directions of $\{W\}$. At every test position, the orientations are iterated by a yaw angle and a pitch angle in increments of 1°. For the given position and orientation of $\{H\}$, the corresponding position of $\{D16\}$ and $\{D24\}$ can be calculated. Then the validness is checked, and the valid pose is counted for the current $r$ and $\gamma$. Under such quantification of the CombX workspace, the optimal configuration possesses the most valid poses.

With the aforementioned quantification of the CombX's workspace, the optimization for maximizing the number of CombX's valid poses was carried out to determine the CombX's arrangement parameters, as shown in (4).

$$[r,\gamma] = \arg\max_{r,\gamma}(\mathrm{PoseNum}_{CombX}(r,\gamma)) \tag{4}$$

Where $\mathrm{PoseNum}_{CombX}(r,\gamma)$ is the number of the valid poses with the given $r$ and $\gamma$.

The arrangement parameters of the CombX, $r$ and $\gamma$, are set within [100 mm, 400 mm] and [60°, 120°] respectively. The relative angle was expected within [60°, 120°], because enough space shall be reserved for the user's hand to manipulate the handle.

The *simulannealbnd* function in MATLAB for simulated annealing algorithm was used to solve the arrangement optimization. The initial values of $[r, \gamma]$ = [200 mm 90°] are used. The results from the *simulannealbnd* function were $[r, \gamma]$ = [149.41 mm 119.99°] with 955714 valid poses. For simplicity of the construction, the two TouchX devices arranged according to the parameters of $[r, \gamma]$ = [150mm 90°] with 936613 valid poses. Since this number of the valid poses is close to the optimum (98% of the optimum), these two values were assigned to the arrangement of the CombX. The workspace of the CombX is then plotted in Fig. 4. A rated workspace of the CombX with a size of 160 × 160 × 160 mm$^3$ is located at [0 mm 0 mm 150 mm]$^T$ in $\{W\}$.

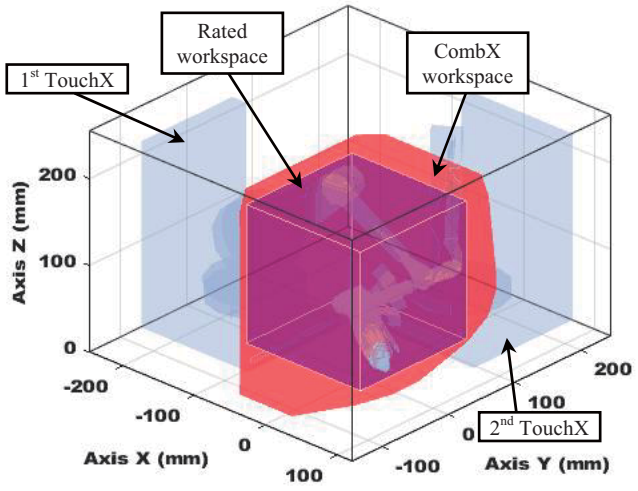


Figure 4. Workspace of the CombX

With the relative position of the TouchX devices determined, the complete kinematics of the CombX can be derived. The base of the 1st TouchX device $\{D10\}$ is located at ${}^{W}\mathbf{p}_{D10}$ = [-150 mm 0 mm 0 mm]$^T$ in $\{W\}$, while the 2nd base $\{D20\}$ is placed at ${}^{W}\mathbf{p}_{D20}$ = [0 mm 150 mm 0 mm]$^T$ in $\{W\}$. Then the homogeneous transformation matrix linking $\{H\}$ and $\{W\}$ can be obtained as in (5).

$${}^{W}\mathbf{T}_{H} = \begin{bmatrix} \mathbf{I}_{3\times3} & {}^{W}\mathbf{p}_{D10} \\ \mathbf{0}_{1\times3} & 1 \end{bmatrix} \cdot {}^{D10}\mathbf{T}_{H} \tag{5}$$

## IV. Preliminary Experimentations

In this section, the preliminary experimentations for quantifying the precision of the translational and orientation workspace were carried out to demonstrate the effectiveness of the CombX.

The experimentations of positioning precision were conducted first. As shown in Fig. 5, the new stylus of the CombX was held and manipulated by a 6-DoF Denso manipulator inside the CombX's workspace. The Denso manipulator can generate the steady and repeatable motions to facilitate the experiments.

The motions of the Denso's end effector and the CombX's new stylus were measured as follows. Two markers were attached to the handle and the base of the CombX respectively. Then a tracker (Micron Tracker SX60 from Claron

Technology Inc.) was utilized to detect the positions and orientations of the markers in $\{W\}$.

The position precision was verified as follows. The Denso manipulator was commanded to move the CombX's handle in the XYZ directions in $\{W\}$ respectively. Via the APIs (Application Programming Interfaces) of the TouchX devices, the joint values of the 1st TouchX device can be obtained. Then, the position and orientation of the CombX's handle can be calculated using (5). Figure 6(a) illustrates these calculated positions of the handle, while Figure 6(b) shows the errors between the actual positions and the calculated positions. It can be seen that these position errors are mostly under 0.10 mm. The datasheet shows that the position resolution of the TouchX device is 0.023mm. The tracker's tracking errors might contribute to the errors.

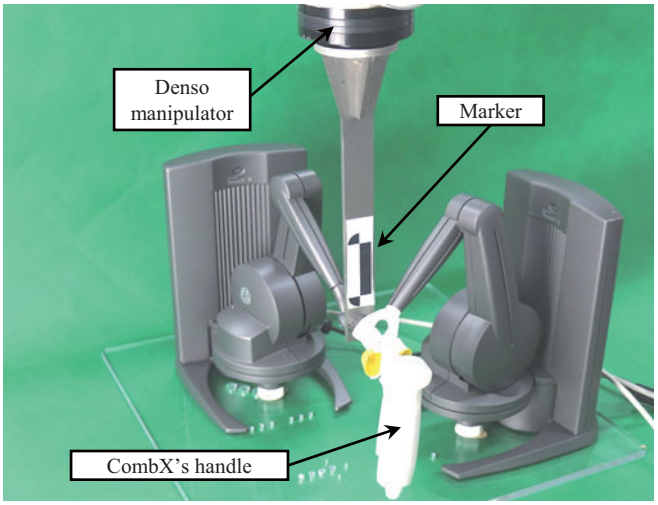


Figure 5. Pose read-outs of the CombX held by a Denso manipulator

Next, the motion capability on the rated workspace of the CombX is demonstrated. The Denso manipulator was commanded to move the handle of the new stylus on the edges of the CombX's rated workspace. The actual positions of the CombX's handle were read by the optical tracker, while the calculated positions were obtained via the joint values from the APIs and the kinematics in Section III. As shown in Fig. 7, it is clear that the CombX has good positioning precision within the rated workspace, because it is commonly considered that the points on the boundaries of the workspace have worse precision.

In the characterization of the orientation capabilities of the CombX, solid angle (in steradian) is applied to quantify the CombX's reachable orientations at different positons (Points A to L in Fig. 9) inside the rated workspace. The reachable orientation is the direction reached by the CombX handle axis $\hat{\mathbf{z}}_H$. The aforementioned solid angle is obtained as follows.

The CombX's handle is maneuvered and oriented passively by the Denso manipulator to different directions, and its position is maintained at the desired position, as shown in Fig. 8. A six-dimensional force sensor (Nano17 from ATI Industrial Automation Inc.) was utilized to confirm the orientation reachability. The reachable direction should satisfy the following conditions: i) the position of the CombX's handle was at the desired point; ii) the forces and the torques measured by the Nano17 were smaller than 0.5 N and 50 mNm. When the orientation is quantified, large forces or torques measured by the Nano 17 sensor always means structural interferences or motion limits were encountered.

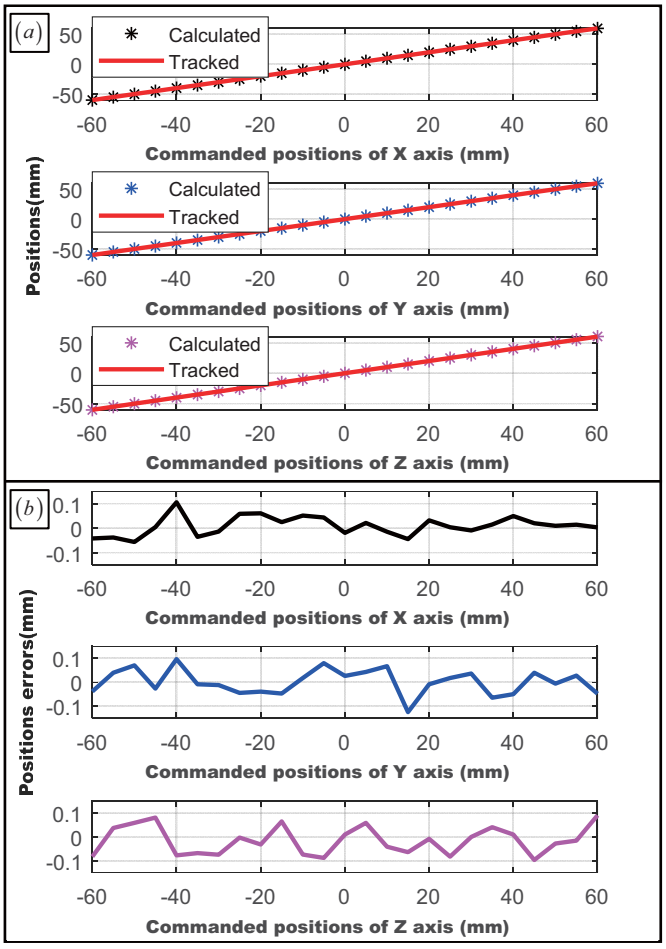


Figure 6. Experimental results: (a) actual and calculated positions, and (b) positions errors

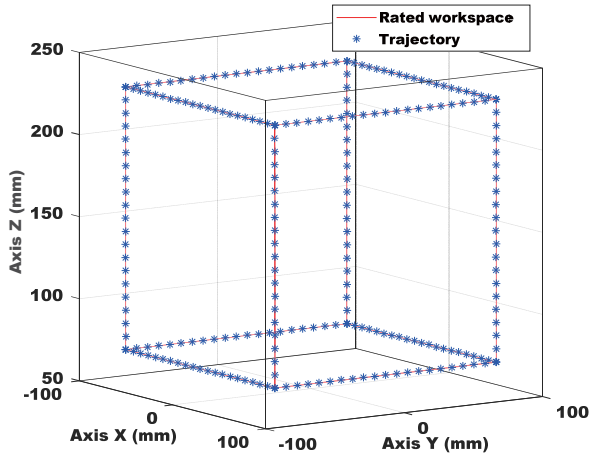


Figure 7. Motion capability experimental results on the rated workspace

The directions can be parameterized by a yaw angle and a pitch angle in increments of 1°. As shown in Fig. 9, the red

patches are the reachable directions of the representative Points (A to L). The center of the rated workspace has the largest orientation workspace (7.04 sr). The original orientation workspace of the TouchX device is 7.07 sr.

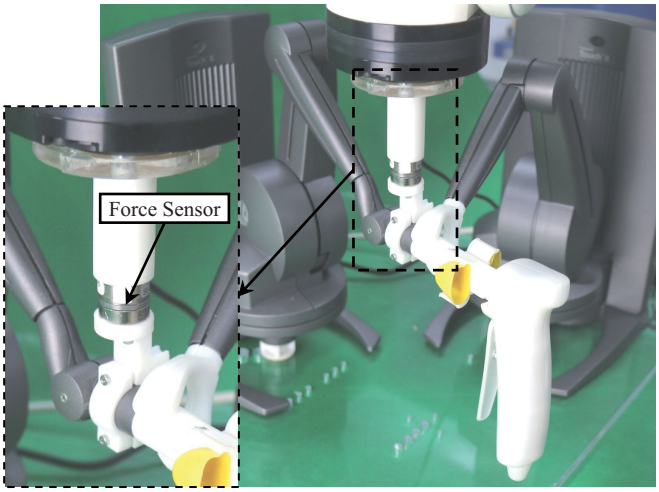


Figure 8. Pose read-outs of the CombX held by a Denso manipulator

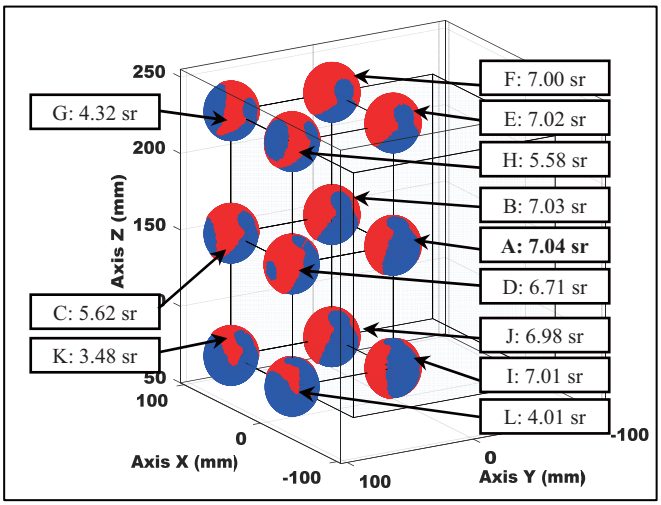


Figure 9. Experimental quantification of the orientaion workspace

## V. Conclusions and Future Work

In order to facilitate the accesses to the haptic devices with both force and torque outputs, the CombX design is proposed. This paper presents the design, construction, arrangement optimization, and preliminary experimentation for the position and orientation workspace of the CombX.

The key innovation is the design of a new stylus to replace the original styluses and connect two TouchX devices. The new stylus was easily fabricated via 3D printing. And most importantly, the integrity of the electronics system of the TouchX devices is fully reserved. The easy-to-use APIs and the product grade reliability facilitate the use of the CombX device in teleoperation tasks. With the two TouchX devices optimally arranged, the CombX fully utilizes the capabilities of the TouchX devices.

Preliminary experiments showed that the CombX has a rated workspace of 160 ×160×160 $mm^3$ with a position sensing accuracy of 0.10 mm. The orientation workspace is up to 7.04 sr.

Next, the wrench outputs specifications of the CombX would be characterized via extensive experimentation in the near future. With the capabilities fully demonstrated, the CombX could become a cost-effective option for haptic devices with both force and torque outputs.

## References


[1] B. Hannaford and A. M. Okamura, "Haptics," in *Springer Handbook of Robotics*. vol. Part D, B. Siciliano and O. Khatib, Eds., ed: Springer, 2008, pp. 719-739.

[2] R. Steger, K. Lin, B. D. Adelstein, and H. Kazerooni, "Design of a Passively Balanced Spatial Linkage Haptic Interface," *Journal of Mechanical Design,* vol. 126, pp. 984-991, 2004.

[3] J. Arata, H. Kondo, N. Ikedo, and H. Fujimoto, "Haptic Device Using a Newly Developed Redundant Parallel Mechanism," *IEEE Transactions on Robotics,* vol. 27, pp. 201-214, 2011.

[4] L. Birglen, C. Gosselin, N. Pouliot, B. Monsarrat, and T. Laliberté, "SHaDe, a New 3-DOF Haptic Device," *IEEE Transactions on Robotics and Automation,* vol. 18, pp. 166-175, April 2002.

[5] G. L. Long and C. L. Collins, "A Pantograph Linkage Parallel Platform Master Hand Controller for Force-Reflection," in *IEEE International Conference on Robotics and Automation (ICRA)*, Nice, France, 1992, pp. 390-395.

[6] Y. Tsumaki, H. Naruse, D. N. Nenchev, and M. Uchiyama, "Design of a Compact 6-DOF Haptic Interface," in *IEEE International Conference on Robotics and Automation (ICRA)*, Leuven, Belglum, 1998, pp. 2580-2585.

[7] L. J. Stocco, S. E. Salcudean, and F. Sassani, "Optimal Kinematic Design of a Haptic Pen," *IEEE/ASME Transactions on Mechatronics,* vol. 6, pp. 210-220, Sept 2001.

[8] M. Ueberle and M. Buss, "Design,Control,and Evaluation of a New 6 DOF Haptic Device," in *IEEE/RSJ International Conference on Intelligent Robots and Systems (IROS)*, Lausanne, Switzerland, 2002, pp. 2949-2954.

[9] K. Kim and W. Kyun, "Design and Analysis of a New 7-DoF Parallel Type Haptic Device: PATHOS-II," in *IEEE/RSJ International Conference on Intelligent Robots and Systems (IROS)*, 2003, pp. 2241-2246.

[10] E. L. Faulring, J. E. Colgate, and M. A. Peshkin, "The Cobotic Hand Controller: Design, Control and Performance of a Novel Haptic Display," *International Journal of Robotics Research,* vol. 25, pp. 1099-1119, 2006.

[11] Z. Najdovski, S. Nahavandi, and T. Fukuda, "Design, Development, and Evaluation of a Pinch–Grasp Haptic Interface," *IEEE/ASME Transactions on Mechatronics,* vol. 19, pp. 45-54, 2014.

[12] G. Lee, S.-M. Hur, and Y. Oh, "A Novel Haptic Device with High-Force Display Capability and Wide Workspace," in *IEEE International Conference on Robotics and Automation (ICRA)*, Stockholm, Sweden, 2016, pp. 2704-2709.

[13] Y. Lin and Y. Sun, "5-D Force Control System for Fingernail Imaging Calibration," in *IEEE International Conference on Robotics and Automation (ICRA)*, Shanghai, China, 2011, pp. 1374-1379.

[14] Y. Kobayashi, Y. Sekiguchi, T. Noguchi, Y. Takahashi, Q. Liu, S. Oguri, *et al.*, "Development of a Robotic System with Six-Degrees-of-Freedom Robotic Tool Manipulators for Single-Port Surgery," *International Journal of Medical Robotics and Computer Assisted Surgery,* vol. 11, pp. 235-246, June 2015.

[15] K. Xu, B. Zhao, S. a. Zhang, Z. Zhang, and N. Xing, "Design of a Haptic Master Device for Teleoperation Applications," in *IEEE International Conference on Robotics and Biomimetics (ROBIO)*, Macau SAR, China, 2017, pp. 1436-1441.